International Journal of Hyperthermia

ISSN: 0265-6736 (Print) 1464-5157 (Online) Journal homepage: informahealthcare.com/journals/ihyt20

Monitoring the effect of mild hyperthermia on tumour hypoxia by Cu-ATSM PET scanning

Robert J. Myerson, Anurag K. Singh, Heather M. Bigott, Bibiana Cha, John A. Engelbach, Joonyoung Kim, Wayne T. Lamoreaux, Eduardo Moros, Petr Novak, Terry L. Sharp, William Straube, Michael J. Welch & Mai Xu

To cite this article: Robert J. Myerson, Anurag K. Singh, Heather M. Bigott, Bibiana Cha, John A. Engelbach, Joonyoung Kim, Wayne T. Lamoreaux, Eduardo Moros, Petr Novak, Terry L. Sharp, William Straube, Michael J. Welch & Mai Xu (2006) Monitoring the effect of mild hyperthermia on tumour hypoxia by Cu-ATSM PET scanning, International Journal of Hyperthermia, 22:2, 93-115, DOI: 10.1080/02656730600594191

To link to this article: https://doi.org/10.1080/02656730600594191

Published online: 26 Aug 2009.

Submit your article to this journal

Article views: 483

View related articles

Citing articles: 2 View citing articles

Full Terms & Conditions of access and use can be found at
https://informahealthcare.com/action/journalInformation?journalCode=ihyt20

Int. J. Hyperthermia, March 2006; 22(2): 93–115

Taylor & Francis
Taylor & Francis Group

Monitoring the effect of mild hyperthermia on tumour hypoxia by Cu-ATSM PET scanning

ROBERT J. MYERSON[1], ANURAG K. SINGH[1], HEATHER M. BIGOTT[2], BIBIANA CHA[1], JOHN A. ENGELBACH[2], JOONYOUNG KIM[2], WAYNE T. LAMOREAUX[1], EDUARDO MOROS[1], PETR NOVAK[1], TERRY L. SHARP[2], WILLIAM STRAUBE[1], MICHAEL J. WELCH[2], & MAI XU[1]

[1]*Department of Radiation Oncology and* [2]*Radiological Sciences, Mallinckrodt Institute of Radiology, Washington University School of Medicine, St. Louis, MO, USA*

(Received 27 December 2004; revised 16 March 2005; in final form 23 January 2006)

Abstract

Purpose: Mild hyperthermia can improve tumour oxygenation and enhance radiosensitivity. Imaging the hypoxic fraction of a tumour can guide hyperthermia treatment planning and facilitate treatment optimization. ^{64}Cu-ATSM (Copper-diacetyl-bis(N^4-methylthiosemicarbazone)) is a positron emitting compound that has been demonstrated to have rapid uptake and selective retention in hypoxic cells and has been used for imaging human and animal tumours. The purpose of the present report is to establish methodology that will allow one to use Cu-ATSM PET scanning to detect the impact of hyperthermia on tumour physiology in as little time as possible.

Materials and methods: EMT6 tumours (mouse mammary carcinoma) were implanted into the subcutaneous tissue of both thighs of 10 BALB/c mice (one heated, one control tumour per animal). The target thermal dose was $41.5^{\circ}\mathrm{C} \times 45$ min. Without interrupting heating, ^{64}Cu-ATSM (mean activity 1.8 mCi) was then injected and serial PET scans were obtained. In a sub-group of four animals, a low administered activity ($\sim$0.3 mCi) ^{64}Cu-ATSM scan was also conducted before heating to permit a direct comparison of the effects of hyperthermia on the same tumours. In another sub-group of five animals, a low activity ($\sim$0.3 mCi) ^{64}Cu-PTSM (pyruvaldehyde-bis(N^4-methylthiosemicarbazone)) scan was conducted before heating, to confirm a posited correlation between perfusion and early ^{64}Cu-ATSM uptake.

Results: This study corrected for perfusion differences by dividing tumour uptake by the average early (first minute) uptake ('self-normalized uptake'). The 10 heated tumours showed a significantly ($p = 0.007$) lower self-normalized uptake than control tumours by 2 min. For the four mice with low activity Cu-ATSM scans performed before hyperthermia, the tumours to be heated demonstrated self-normalized uptake consistent with the unheated control tumours and which departed significantly ($p \leq 0.02$) from their post-hyperthermia scans by 5 min. Comparisons between scans and needle electrode surveys were performed in an additional four animals with eight tumours. For technical

Correspondence: Robert J. Myerson, MD, PhD, Radiation Oncology Department, Washington University School of Medicine, 4921 Parkview Place, Lower Level, St. Louis, MO 63110, USA. Tel: 314-362-8503. Fax: 314-747-9557. E-mail: myerson@radonc.wustl.edu

ISSN 0265–6736 print/ISSN 1464–5157 online © 2006 Taylor & Francis
DOI: 10.1080/02656730600594191

reasons electrode surveys were done after the end of hyperthermia—and, therefore, these animals also had comparison scans taken after hyperthermia. Reduced self-normalized uptake on scans was associated with increased pO_2 on electrode surveys. These data also suggested a substantial degradation of the effect on tumour hypoxia by ~15–45 min after the end of mild hyperthermia.
Conclusion: Short imaging times of ~5 min with modest (~4–10) numbers of mice can discriminate the effects of mild hyperthermia on tumour physiology. The long-term objective is to use this tool to identify as short and mild a hyperthermia session as possible.

Keywords: *Hyperthermia, hypoxia, Cu-ATSM PET imaging*

Introduction

An important mechanism by which mild hyperthermia can improve the response of tumours to radiation therapy is by reducing hypoxia [1–7]. Although higher temperatures can cause vascular shutdown with reduced perfusion and increased hypoxia [7], milder temperatures (below ~42°C) will typically stimulate perfusion in the tumour and improve oxygenation [4, 6, 8, 9]. In addition, temperature elevation will reduce the oxygen binding of haemoglobin, contributing to increased delivery of oxygen within a region of localized hyperthermia [10]. The time course of these changes can be complex with some observers noting the peak effect during [4, 11] or ~2–15 min after [6, 8, 9]. Others note that the effect can be present 1 day after [2, 7] mild hyperthermia. In one study, the time course of changes in tumour oxygenation was also temperature dependent, with higher thermal dose improving oxygenation in a delayed fashion [6].

The typical way that oxygenation status is monitored is by multi-point measurements with needle electrodes [12, 13]. There are several disadvantages to this approach. Estimates of pO_2 distribution are subject to sampling errors. In small animal tumours the physical destruction from moving a needle probe can distort the local micro-environment. In humans, needle probes constitute another uncomfortable invasive procedure for the patient who usually is being treated with palliative intent. The time needed for adequate needle sampling can limit the ability to investigate transitory, short duration effects. It is technically difficult to perform aggressive multiple location electrode measurements during a hyperthermia session, so that, for the most part, the literature is confined to assessing effects on oxygenation after hyperthermia is completed. Finally, electrode measurements evaluate the volumetric pO_2 distribution, rather than the proportion of viable tumour cells that are hypoxic. If there is over-sampling of a necrotic core or under-sampling of the zone of hypoxic but viable tissue surrounding it, the electrode measurements could, respectively, over- or under-estimate the hypoxic fraction.

There are several imaging modalities in development that offer the promise of obtaining information about the whole tumour's oxygenation status [14–23]. One approach is positron emission tomography (PET) scanning using the radiotracer Cu(II)-diacetyl-bis (N^4-methylthiosemicarbazone) (Cu-ATSM) [21, 24, 25]. Cells under hypoxic conditions ($pO_2 < \sim 5$ mm Hg) are markedly more likely to retain the Copper than normoxic cells [25]. Using a suitable positron emitting isotope of Copper, Cu-ATSM PET scanning will show greater intensity in regions of hypoxic but viable cells [21, 25]. For studies in humans the short half-life isotope ^{60}Cu is used [26–29]. For small animal studies, ^{64}Cu is preferred because its lower energy positron permits spatial resolution on the order of a millimeter [21, 30]. One prefers Cu-ATSM PET scanning because its uptake within hypoxic cells is rapid, reaching a substantial level within 15 min or less [25]. This rapid uptake makes it feasible to use Cu-ATSM PET scanning to monitor effects that could change within minutes (which may be an advantage over nitroimidazole scanning, where rate

of uptake is slower). In addition, the information obtained from Cu-ATSM scans relates directly to the fraction of viable but hypoxic cells, in contrast to magnetic resonance imaging approaches (which provide information about the overall distribution of oxygen within the tumour, but do not directly identify hypoxic but viable regions). As with other PET-based approaches, both small and large animals including humans can be imaged. A number of clinical investigations have shown strong correlations between Cu-ATSM PET scan findings and treatment outcome for a variety of human malignancies including head and neck cancers [27], gynecologic malignancies [28] and lung cancers [29].

Hyperthermia is also a useful test intervention, to evaluate how best to utilize a hypoxia imaging modality. Because hyperthermia can be localized, it is possible to compare a heated tumour with an unheated control tumour in the same animal. This can be helpful in determining how best to extract information from the PET scans.

The purpose of the present study is to develop a technique for using Cu-ATSM PET scanning to rapidly discriminate the impact of mild hyperthermia. The long-term goal is to optimize the thermal dose for clinical purposes. However, in the present study, the thermal dose consists of 41.5°C maintained for ~45 min. This is a regimen which has been shown to improve oxygenation [4, 6, 8, 9], produces little or no direct cell kill on its own (although heat induced radiosensitization can occur [31–38] and will serve as a fairly well understood prototype for evaluating the effects of a hypoxia directed intervention on Cu-ATSM scans. This may not necessarily be the clinically optimized regimen. A much shorter heating session might eventually be more convenient in the clinic and—if the target temperature is still 41.5°C—can safely be conducted with less invasive thermometry than a longer session at the same temperature (because there is less time for unexpected high thermal dose locations to develop and cause injury). The optimal session might also be one that is extremely short and has a very transitory effect on tumour oxygenation. For example, radiation and hyperthermia can be given simultaneously [39–41]. If it proves to be the case that the oxygenation improvement from a very short session reverses shortly after cessation of hyperthermia/radiation, then inter-treatment repopulation among hypoxic but viable cells will be less than if they remained oxygenated between treatments—a potential therapeutic advantage. For these reasons, the objective is to find a way to discriminate the impact of hyperthermia on PET scans in as little time as possible and without interrupting heating. The purpose of the present paper is to establish such a measure for utilizing Cu-ATSM PET scan information.

In using a PET-based approach, it is important to understand that the intensity of uptake is determined not only by how well the cells retain the radiotracer but also by how well they are supplied with it. Evaluating an intervention, like mild hyperthermia, that increases local perfusion, needs to be done in a fashion that accounts for the effects of enhanced radiotracer delivery on uptake patterns.

Methods and materials

Prior to *in vivo* animal testing, the *in vitro* uptake of Cu-ATSM by EMT6 mouse mammary carcinoma cells was evaluated at 0% oxygenation, under conditions of mild hyperthermia and normothermia. This was done to make certain that hyperthermia itself does not reduce radiotracer uptake independent of change in oxygenation. The methodology of Lewis et al. [25] was used. Cell suspensions were continuosly stirred, maintained within ±0.5°C of target temperature and kept at controlled oxygen tension for 45 min, after which ~30 μCi radiolabelled ^{64}Cu-ATSM was added to the suspensions. Target temperature

continued to be maintained. Multiple aliquots were taken at $t = 1.7, 7.5, 15, 30$ min after administration of Cu-ATSM. The cells were pelleted from the media and the percentage uptake (pellet/(pellet + supernatant)) was calculated.

The animal tumour model for these studies was the EMT6 mouse mammary carcinoma implanted in the lateral aspect of the proximal hindlimbs of 10 BALB C mice. These tumours have been shown to develop hypoxic regions at modest size [42–44]. Their *in-vivo* Cu-ATSM uptake has been reported previously [25]. A tumour was implanted in each hindlimb (two tumours per mouse), one to be heated and the second to serve as an unheated control. Tumours were grown for a period of 1.5–2 weeks until they attained a diameter of ~1 cm before PET scanning and hyperthermia.

PET scanning and hyperthermia sequences

The PET scanning protocol was as follows. Animals were anaesthetized with isofluorane and were provided with room air by mask inhalation. A jugular venous catheter for radiotracer administration was placed. A thin flexible thermocouple probe (Physitemp Corp, Clifton, NJ) was inserted into the tumour to be heated through a needle puncture track and sutured in place with a small skin suture. An additional flexible thermocouple probe was placed in the rectum for systemic temperature monitoring. One or two animals were positioned on a tray designed to permit simultaneous hyperthermia and PET scanning in the bore of the MicroPET R4 (Concorde Microsystems, Knoxville, TN) scanner. Prior to hyperthermia, nine of the 10 animals underwent a low administered activity (0.17–0.7 mCi, average 0.3 mCi) scan for several auxiliary purposes (discussed below). The intention was to use as low an administered activity as possible and have sufficient image quality to identify volumes of interest. The first two animals scanned had low activity scans with administered activities of 0.7 and 0.36 mCi. After establishing that image quality was adequate at the lower level, all subsequent low administered activity scans were with ~0.2–0.3 mCi.

Following the low-activity scan, localized hyperthermia was begun on one of the two tumours on each animal (techniques discussed below) with the control tumour remaining unheated. The target hyperthermia session was 45 min at 41.5°C. However, when two animals were treated at the same time, inevitably one tumour would reach target temperature ahead of the other. The minimum and maximum time at or above 41°C were 30 and 60 min, respectively, preferably with both tumours as close to 45 min as possible. After target time was reached, the second, higher administered activity (1.4–2.0 mCi, average 1.8 mCi), PET scan was initiated without interrupting hyperthermia. The full activity scan was a ^{64}Cu-ATSM scan for all 10 animals. Throughout this scan, the heated tumours were maintained at 41.5 ± 0.5°C. Rectal temperature was kept to 36 ± 3°C using heating lamps or a cooling fan as needed throughout the process. After PET scanning and hyperthermia and while still under anaesthesia, all mice were sacrificed by cervical dislocation.

The image acquisition protocol for both high and low activity scans was as follows: images were captured every 5 s after injection for the first minute, followed by every 30–60 s for 9 min, followed by every 60–300 s for 10–35 min (total scan time 20–45 min). For a given animal, the same image acquisition protocol was used for both the pre- and post-hyperthermia scans. Image processing software was used to reconstruct 1 mm axial, coronal and sagittal sections displaying distribution of radiotracer throughout the animals with a voxel size of $0.8 \times 0.8 \times 1$ mm.

Hyperthermia techniques

Two heating techniques were utilized. The first five animals studied were heated by thermal conduction. Design constraints for the hyperthermia applicator were (i) that the device fit inside the bore of the MicroPET with easy access, (ii) two mice could be heated and scanned at the same time, (iii) no free water or other spillable liquid within the MicroPET bore, and (iv) no elements that could severely attenuate the photons produced by positron decay. The design consisted of a plastic chamber (28 mm inner diameter (ID) × 35 mm deep) surrounded in its upper 1.5 cm by a plastic tubing coil (3 mm ID) mounted on a Plexiglas platform (Figure 1). This coil was insulated with foam-tape and connected via larger plastic tubing (6.4 mm ID) to a heat exchanger coil of copper tubing also of 6.4 mm ID. The heat exchanger was inserted as needed into a temperature controlled water bath (not shown). The tumour to be heated was positioned 1 cm from the chamber's top. The chamber was then filled with pre-heated electrode cream (sigma crème, Parker Labs, NJ) that served as the thermal conductive, non-spillable medium. Heated water was circulated through the tubing by a peristaltic pump and warmed the chamber. Tumour temperature was controlled by adjusting the water bath chamber (between 45–50°C) and by removing the heat exchanger coil as needed from the water bath. Because of thermal conduction losses in the connecting tubing, the water bath temperature was higher than the temperature of the conducting cream in the plastic chamber or the animal's leg. The thermal conduction system, although labour intensive, was able to maintain tumour temperature within 0.5°C (usually within 0.2°C) of 41.5°C.

Heating for the last five animals studied was done by an external ultrasound device, SAHUS or small animal hyperthermia ultrasound system, which has previously been described [41]. This system utilized a small ultrasound transducer to heat tumour in the lateral hindlimb (Figure 1). Uniformity of heating, accounting for thermometry artifacts and microPET compatibility have been discussed in a previous publication [41]. This system included automated power control to maintain target temperature, which made

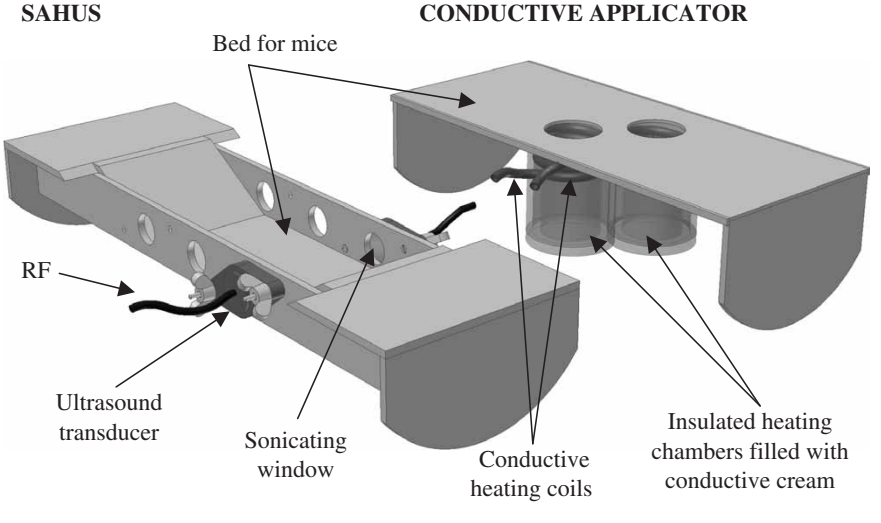

Figure 1. Schematic for heating configuration: conductive approach (first five mice), ultrasound approach (last five mice). See text. SAHUS indicates the Small Animal Hyperthermia Ultrasound System.

it far less labour intensive than the conduction system—which motivated the change in heating approach. In addition it was able to reach target temperature quicker than the conduction system, with small animal tumours reaching 41°C within 5 min.

Uniformity of temperature over time for the two heating systems was similar. Temperature at the surface of the tumour remained within 0.5°C of temperature at the tumour core for the ultrasound system. With the conductive system, the surface temperature ranged up to 1°C above or below tumour core temperature (depending on whether the heat exchanger was in or out of the water bath) with an average difference of +0.4°C.

Mice heated by thermal conduction were prone with the heated limb hanging into the chamber and the unheated control flat on the surface of the tray. When two mice were heated their heads were facing in opposite directions. With the SAHUS the heads faced in the same direction and the animals were supine.

Low administered activity pre-hyperthermia scanning

Low administered activity, pre-hyperthermia, scans were done on the first four and last five animals. For the first four mice, the low activity scan was also with ^{64}Cu-ATSM. The subsequent heating for these four mice was by the thermal conduction system. Comparison of the pre- and post-hyperthermia ATSM scans allows one to directly verify that the intervention produced change in the heated tumours and that, before hyperthermia, the scan properties of the tumours to be heated were similar to the control tumours.

For the last five animals, the low activity, pre-hyperthermia scan was with ^{64}Cu pyruvaldehyde-bis(N*-methylthiosemicarbazone (^{64}Cu-PTSM). The uptake of Cu-PTSM in cells is independent of pO_2 [25]. The distribution of radiotracer in a Cu-PTSM scan is, therefore, considered to be indicative of perfusion. These low activity scans were obtained in order to test the posited association between Cu-ATSM uptake in the first minute after injection and tumour perfusion (discussed below) which were developed after analysis of the first group of animals. The heating for these last five animals was by ultrasound.

Comparison with pO_2 electrode readings

To confirm that, in this animal model, the scan changes are tracking the impact of mild hyperthermia on hypoxia, needle electrode surveys (with comparison scans) were performed. An additional four animals with eight tumours (four heated, four unheated) were studied. It was not technically possible to conduct the electrode readings during hyperthermia or during PET scanning, because of lack of space for the needle electrode/pullback apparatus when the animals were in the heating/scanning tray. Therefore, electrode surveys were conducted as soon as possible after cessation of PET scanning and hyperthermia. A complex sequencing of image times was used, because the evolution of the physiologic effects of hyperthermia during the first ~15–45 min after stopping heat is not known and cannot be assumed to change slowly. Therefore, several post-hyperthermia time points were assessed by scan and electrode.

There were two scan sessions with subsequent electrode surveys, with two animals and four tumours per session. Tumours on these animals were given 41.5°C hyperthermia using the ultrasound system. Low administered activity scans were taken during hyperthermia. Full administered activity scans were taken immediately after (two tumours) or 15 min after (two tumours) the end of hyperthermia. The following scan sequence was used: the mouse on the left side of each tray began heating first. Fifteen minutes after that, heating of the right mouse began. After another 15 min, a low activity of ~0.3 mCi ^{64}Cu-ATSM was

administered to the left mouse. After another 15 min, another ~0.3 mCi ^{64}Cu-ATSM was administered to the right mouse and hyperthermia to the left mouse was halted. After another 15 min, hyperthermia to the right mouse was halted and ~2 mCi ^{64}Cu-ATSM was administered to each mouse. After another 15 min of scanning, the animals were removed from the micro-PET and 11–12 pO_2 readings by successive 1 mm pullbacks along a single needle track were taken, using an Oxylite (Oxford Optronix) pO_2 probe and a mounted micrometer. The heated tumour on the right mouse was surveyed first, followed by the left heated tumour and the two control tumours. Care was taken to survey along a horizontal track through the centre of each tumour, with the tracks to be surveyed positioned as close as possible to the centre of the micro-PET bore during scanning (using aligning lasers). Sufficient time was allowed (typically ~1.5 min) at each dwell point for the pO_2 readings to equilibrate. The total time for electrode surveys averaged 17 min per tumour.

Thus, low administered activity scans were obtained during hyperthermia (beginning 30 min after initiating hyperthermia) for each mouse. The full administered activity scan was obtained immediately after cessation of hyperthermia for the right mouse and 15 min after cessation of hyperthermia for the left mouse. The electrode survey of the right heated tumour began 15 min after cessation of hyperthermia. Since the electrode surveys took ~15 min to complete and since the right mouse's heated tumour was surveyed first, the left mouse's heated tumour was surveyed $\geq$45 min hyperthermia.

The Oxylite probe provided simultaneous temperature and pO_2 readings. Since temperatures revert back to baseline very rapidly after cessations of heating, there was no significant difference between the temperatures of heated and control tumours at the time of during the electrode surveys ($22.3 \pm 0.7^{\circ}$C and $21.0 \pm 0.7^{\circ}$C, respectively).

Volumes of interest

Images were produced using software provided by the manufacturer (ASI Pro, Concorde Microsystems, Knoxville TN) as well as in-house software. The software calculates decay corrected activity in nCi/cc for each voxel within a volume of interest (VOI). In the present study the total uptake in the two thigh tumours for each animal were tracked (Figure 2). The tumour VOIs were drawn to encompass the entirety of the involved thigh without extending into other structures. For this purpose a series of rectangles over seven-to-nine transverse slices were specified. The tumour volume was most easily identified on the last image obtained after injection (a 5 min average obtained at least 20 min after injection of radiotracer). Uptake within the same volume for earlier times was generated automatically.

In addition to the tumours, activity within the heart was tracked as a means of estimating the time dependence of circulating radiotracer. Late coronal images were used to identify the left diaphragm. Early images (0–15 s after injection) were then used to track the bolus of radiotracer from the jugular vein into the ventricle just above the level of the diaphragm. The target volume was a small central sub-volume of the early cardiac uptake (0.06–0.12 cm^3) intended to be small enough to be dominated by radiotracer within the chamber of the ventricle, rather than the muscular walls. This was best identified on early images ~10–15 s after injection, when radiotracer had passed into the heart, but before the uptake in non-vascular thoracic structures developed. Activity vs. time within this volume was then automatically generated. In the present paper, the cardiac information is used only for qualitative purposes.

(a)

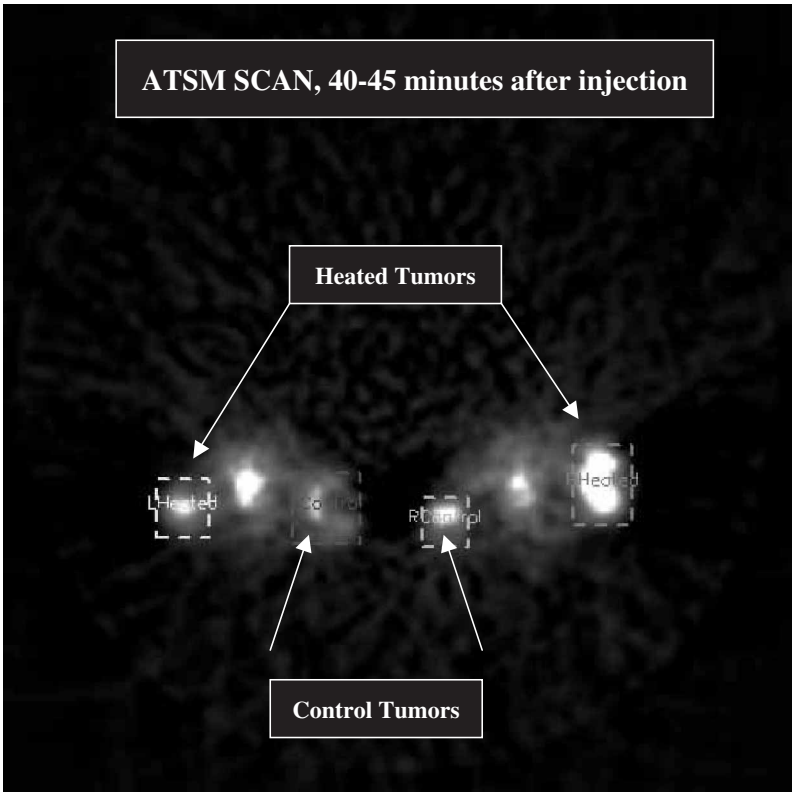

Figure 2. (a) Transverse section from full activity ATSM scan, 5 min average obtained 40–45 min after injection. This image shows two mice at a level that sections through the tumour bearing thighs and the pelvic floor. The lateral thigh tumours are receiving hyperthermia, the medial thigh tumours are unheated controls. The structure between the thigh tumours is the pelvic floor and bladder. Volumes of interest (the heated and control tumours) are displayed. The brightest portions of both control tumours were off this plane, hence the heated tumours display greater uptake in this image. (b) Early ATSM (first minute after injection, 1 min average) for the same two animals shown in (a). (c) Low activity PTSM scan obtained 40–45 min after injection (5 min average) for the same two mice, prior to hyperthermia. Note that the pattern of uptake in the PTSM scan is similar to the early ATSM uptake except for greater early ATSM activity in the two heated tumours, consistent with increased perfusion leading to greater early delivery of radiotracer to the heated tumours.

Four animals had electrode readings after completion of hyperthermia and scanning. For these, the region of interest was a thin ($\sim$1 mm $\times$ $\sim$11 mm) rectangle placed horizontally in a single axial slice at the centre of the tumour, as close as possible to where the electrode survey was planned. An example is given in Figure 3. The ASI Pro software was used to generate uptake profiles across these rectangles for every time frame.

Results

In-vitro *Cu-ATSM uptake and retention*

In-vitro uptake of Cu-ATSM at $41 \pm 0.5^{\circ}$C and $37 \pm 0.5^{\circ}$C is shown in Figure 4. Note that the percentage (y-axis) in this figure is percentage of administered radiotracer,

(b)

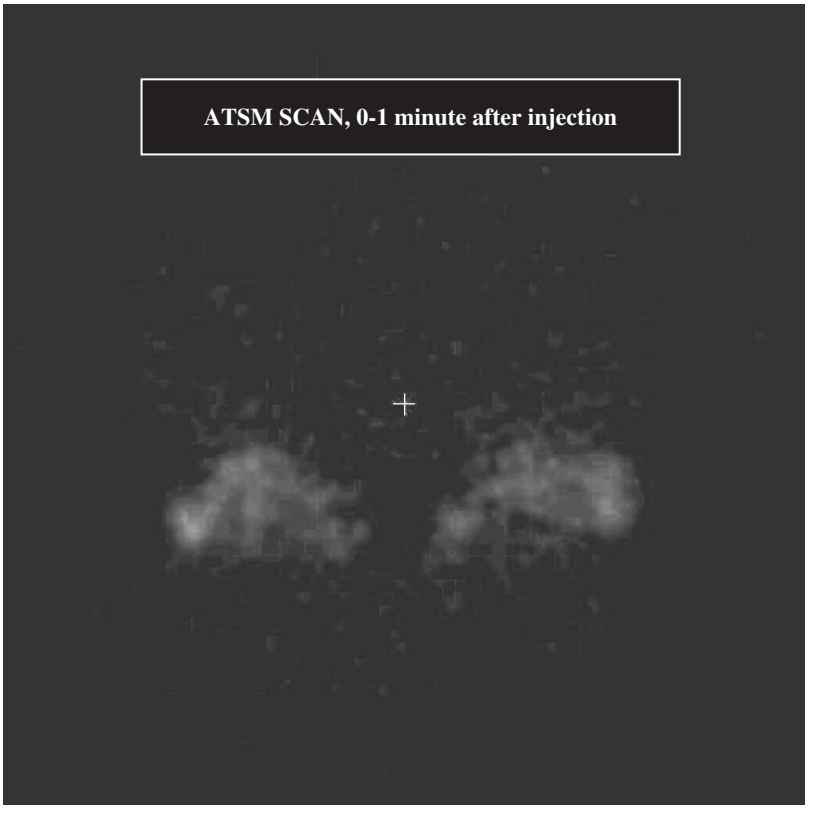

Figure 2. Continued.

not percentage of cells. The actual percentages are, therefore, of less significance than how they change with time, temperature and oxygen tension. This figure shows that, at 0% O_2, retention of Cu-ATSM was greater for 41°C heated cells than for 37°C cells at the same pO_2. This experiment was repeated at 0.5% O_2 and obtained substantially lower uptake. At 30 min the uptake was 0.2 ± 0.02 of the uptake at 0% O_2 for both temperatures. Thus, the uptake in heated cells at 0.5% O_2 is much less than that for unheated cells at 0% O_2.

Note that the *in-vitro* studies were done with a heating schedule that matched the *in-vivo* scanning: 45 min of heating, followed by Cu-ATSM administration. The *in-vitro* studies show that, for this cell line, any intra-cellular effects of the delivered thermal dose led to an *increased* retention of radiotracer, when compared with unheated cells. Since intra-cellular effects increased retention, if evidence is found of *decreased* retention *in-vivo* with hyperthermia, it must be due to changes in the extra-cellular environment (most likely increased pO_2, although conceivably other physiologic effects of hyperthermia could contribute).

In-vivo *scan data*

For the full administered activity scans it is important to correct for any tumour activity left over from the low activity pre-hyperthermia scan (performed on nine of the 10 animals). This was done by subtracting tumour uptake at the time of the second injection from all

(c)

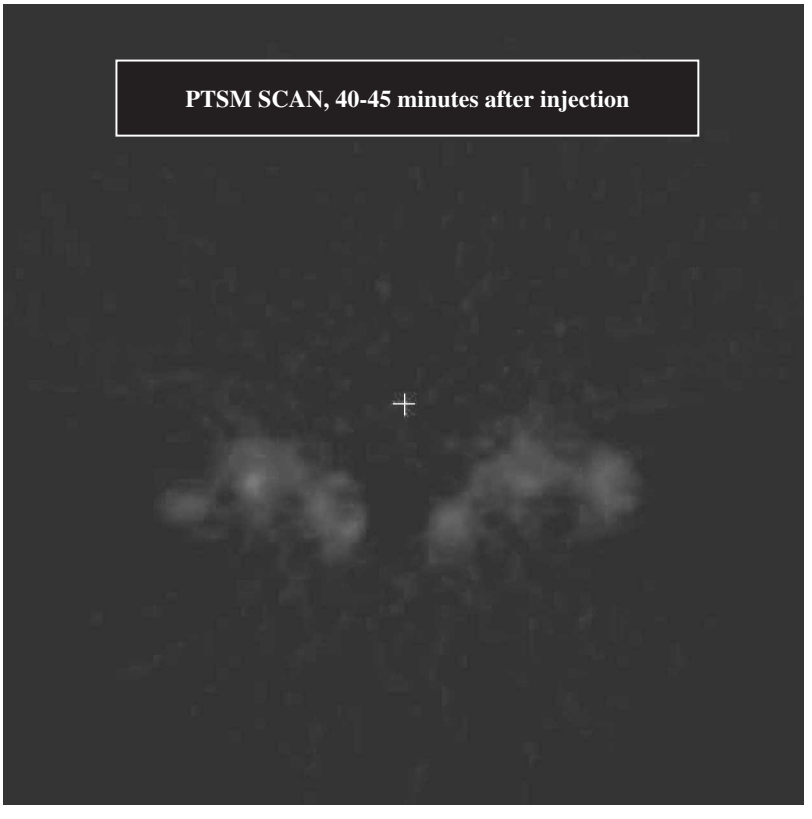

Figure 2. Continued.

subsequent high activity scans. It is assumed that subsequent time dependence of the residual activity is small compared to its value at the time of the second injection. At the time of the second injection, at least 50 min had elapsed since the first, low activity injection (at least 20 min scan time during the first set of scans followed by at least 30 mins for hyperthermia); tumour uptake of radiotracer tends to evolve slowly by then (see Figures 5, 9–11). The fact that the first scan was of lower activity than the second also makes it more tenable to ignore time dependence of residual uptake. As a check on this, tumour uptake at the end of the first scan was compared with uptake at the time of injection for the second scan (with $\geq$30 min of hyperthermia intervening). The residual uptake at the time of the second injection was $95\% \pm 6\%$ of the uptake at the end of the first scan (averaged for 18 tumours in nine mice that had two scans). This 5% change, over 30+ min, in residual uptake from the first, low activity, scan amounted to 0.5% of the average activity taken up by the tumour during the next minute after the second, full activity, ^{64}Cu-ATSM injection.

An example of ^{64}Cu-ATSM activity in heated and control tumours for one animal is displayed in Figure 5. In the first minute after administration of radiotracer there is greater activity in the heated tumour. However, by 4 min the curves have crossed and there is greater long-term activity in the unheated control tumour.

Because of variations between tumours, the absolute uptake at the end of observation was not always less in the heated tumours. However, in the four animals that had low activity ^{64}Cu-ATSM scans prior to hyperthermia, it was possible to correct for any pre-treatment

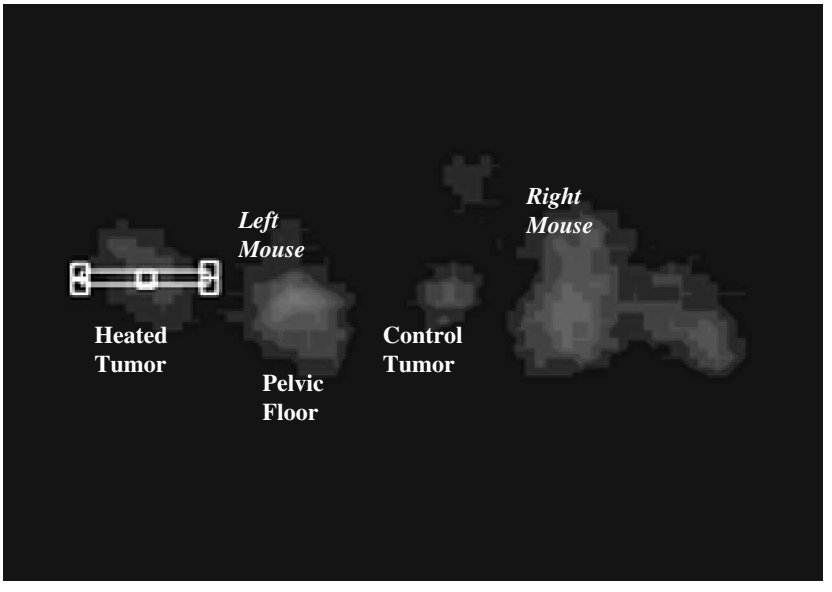

Figure 3. Narrow rectangular region of interest taken through the centre of the heated tumour of the left mouse in Figure 2. Scan uptake profiles within tumours were compared with needle electrode readings along a track positioned as closely as possible to the image profile.

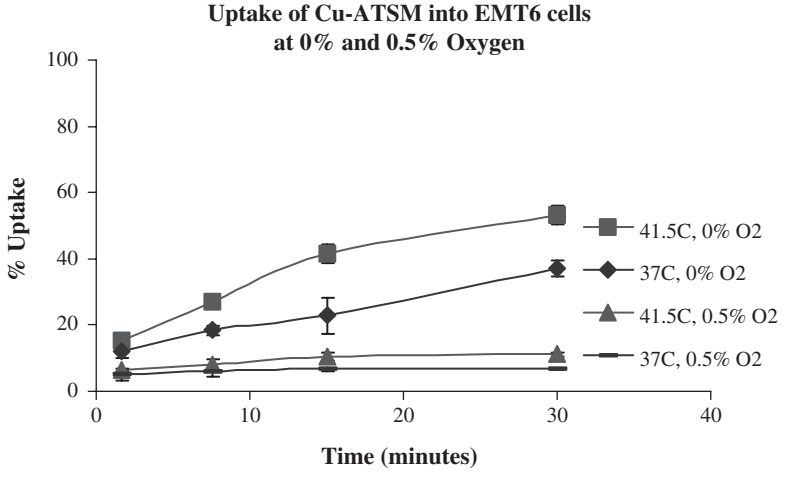

Figure 4. *In-vitro* uptake of Cu-ATSM for EMT 6 cells under hypoxia (0% O_2) and 0.5% O_2, with and without hyperthermia. The methodology of Lewis et al. [25] was used. Cell suspensions were continuosly stirred and maintained at target temperature for 45 min, after which radiolabelled Cu-ATSM was added to the suspensions. Target temperature continued to be maintained. Multiple aliquots were taken at $t = 1.7, 7.5, 15, 30$ min after administration of Cu-ATSM. The cells were pelleted from the media and the percentage uptake (pellet/(pellet + supernatant)) was calculated. Error bars represent standard deviation over three aliquots taken at each time point.

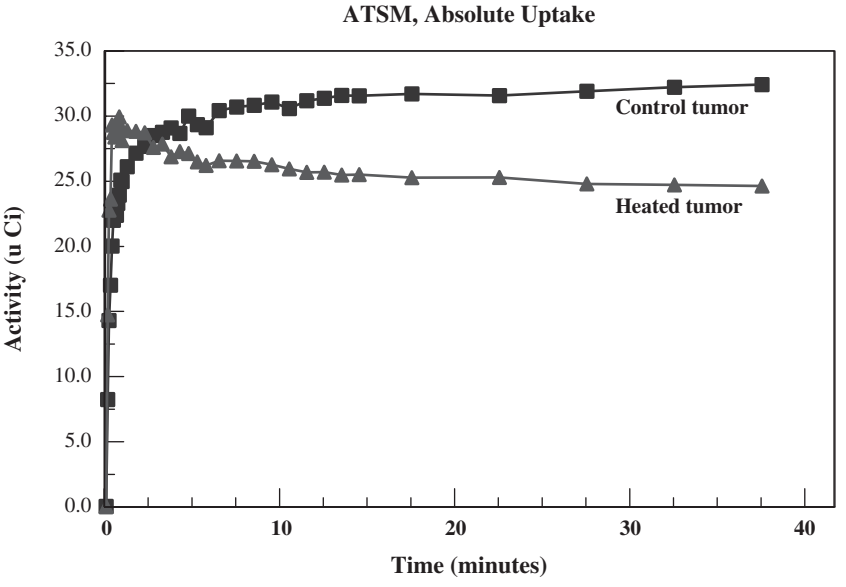

Figure 5. Activity (in micro Curies) *vs.* time after administration of ^{64}Cu-ATSM for a typical case. The heated tumour (triangles) shows greater early uptake than the unheated control tumour (squares). This reverses by 4 min.

differences in tumour oxygenation. For example, in two of the four mice, the low activity scans showed greater uptake in the tumours to be heated than in the control tumours. Baseline differences between the tumours can be accounted for by dividing tumour uptake in the post-hyperthermia scan by uptake in the pre-hyperthermia scan at the same time post-injection. Thus normalized, the ratio of activity between heated and control tumours peaked within the first minute for all four mice and exceeded unity for three of the four mice. By 8 min, however, this heated to control ratio (normalized to pre-hyperthermia ATSM uptake) became less than unity for all four animals.

The long-term plans include scenarios in which one would wish to use other compounds besides ATSM for the low activity, pre-hyperthermia scan. Therefore, one seeks a normalization that does not require a pre-hyperthermia ATSM scan.

Figure 6 shows the average activity within the ventricle vs. time (in units of mCi/cc divided by the total administered activity in mCi). This demonstrates that a large amount of radiotracer leaves the great vessels over the first minute: the decrease in activity within the ventricle from its peak value of $0.24\,\mathrm{cc}^{-1}$ at $t = 12.5$ s to $0.11\,\mathrm{cc}^{-1}$ at $t = 60$ s is more than 2.5 times the subsequent decrease from $t = 60$ s to $t = 45$ min. This means that peripheral structures (including tumours) would be expected to have relatively more activity in the extra-cellular compartment during the first minute than later. This is because, even if there is very rapid transfer into the intra-cellular compartment, the local micro-vasculature is rapidly being re-supplied during the first minute. The average rate of egress from the great vessels between $t = 12.5''$ and $t = 60''$ is more than $2.5 \times 60 \times 44/(60 - 12.5) = 139$ times the average rate after the first minute.

This study uses the average uptake over the first minute as an approximate measure of tumour perfusion. The selection of a 60 s average is an admittedly somewhat arbitrary balance between competing considerations. Shorter lengths of time would sample earlier

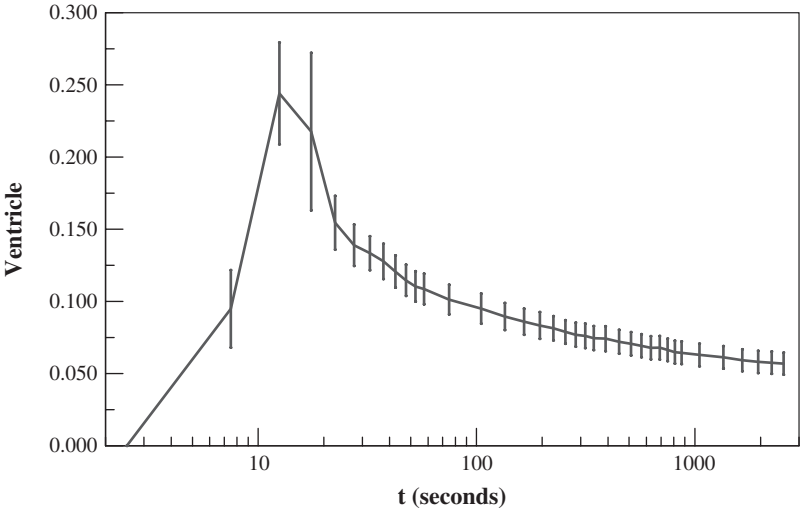

Figure 6. The activity within the chamber of the ventricle *vs*. time (in units of mCi/cc divided by the total administered activity in mCi). Time t denotes time following administration of ^{64}Cu-ATSM. Displayed data are averaged over all mice ± standard error.

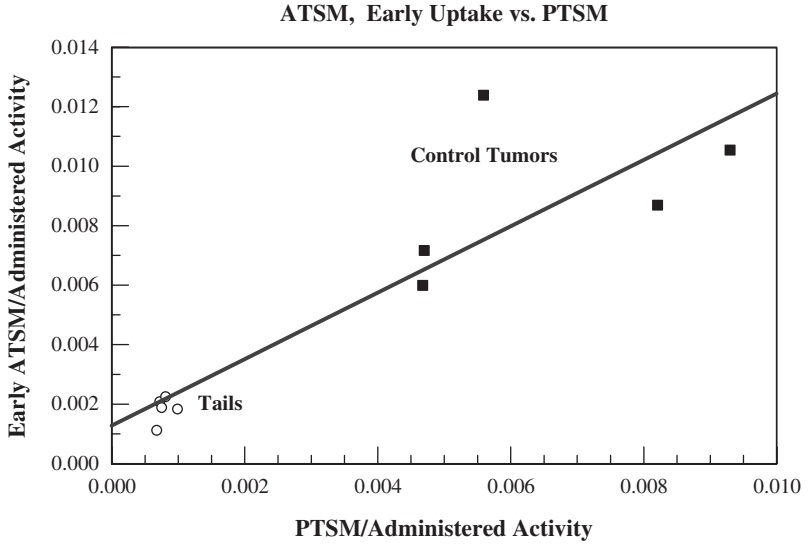

Figure 7. Data from the five mice who underwent low activity Cu-PTSM scans before undergoing hyperthermia and full activity Cu-ATSM scans. The total ^{64}Cu-ATSM uptake averaged over the first minute after administration is compared with the low activity ^{64}Cu-PTSM uptake averaged over a 5 min interval from $t = 40$–45 min. Uptakes are divided by the total administered activity. Shown are data for the five unheated control tumours (squares) and the last 5 mm of the five animals' tails (open circles).

in the perfusion-dominated phase and, therefore, might have less contribution from intracellular uptake. However, averaging over shorter times would have greater measurement uncertainty since there would be fewer positron decays contributing to scan information. In practice, for the 10 animals scanned, the ratio of the early average uptake between

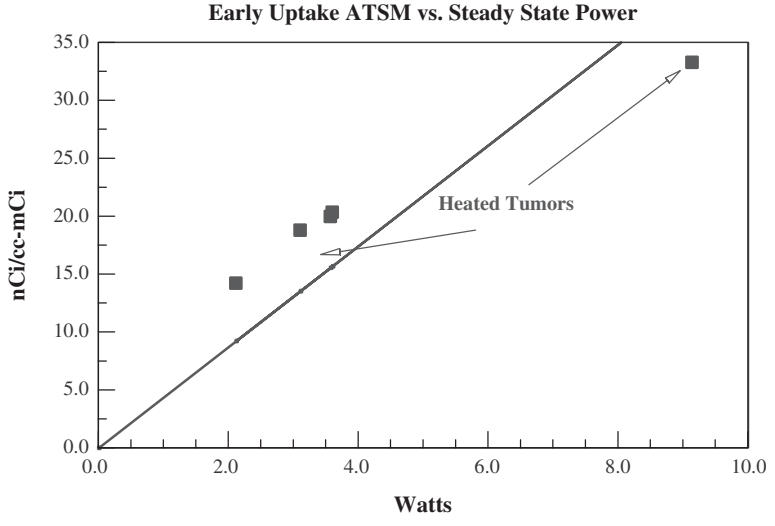

Figure 8. Data for the five tumours heated with ultrasound (same five animals in Figure 7). Displayed is the early uptake (averaged over the first 60 s) of ^{64}Cu-ATSM per cc of tumour *vs*. the steady state ultrasound power needed to maintain temperature at 41.5°C.

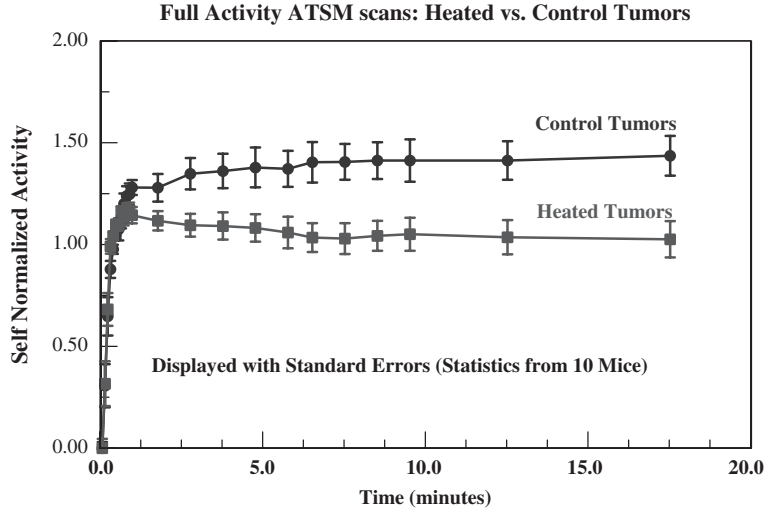

Figure 9. Data from full activity Cu-ATSM scans for all 10 mice. The 'self-normalized' activity is defined to be the activity at a given time after administration of radiotracer divided by the average uptake during the first minute after administration. This is intended to correct for greater perfusion (and, therefore, greater delivery of radiotracer) in heated tumours. Displayed are the average self-normalized uptake ± standard error in heated (squares) and control tumours (circles). The heated and control tumours separate by more than the sum of standard errors by 2 min.

heated and control tumours changed very little between $t = 30$ s and $t = 60$ s (from 1.57 ± 0.18 to 1.48 ± 0.16). The comparisons that follow, between heated and control tumours, would not have been changed if a shorter early average had been selected to normalize for perfusion. The greater early uptake in heated tumours is consistent with

greater perfusion in heated tumours than control tumours. Mild hyperthermia is known to produce increased perfusion [4, 6, 8, 9] and, therefore, would be expected to increase the early delivery of any radiotracer to the heated volume.

We considered several checks of the hypothesis that the early 60 s uptake is approximately proportional to local tumour perfusion. For the five animals that had a low activity ^{64}Cu-PTSM scan, unheated entities (including the control tumour) should show early ^{64}Cu-ATSM uptake that is approximately proportional to the asymptotic level of PTSM uptake, since PTSM uptake is a marker of tumour perfusion. In Figure 7, the total ^{64}Cu-ATSM uptake averaged over the first minute after administration is compared with the low activity ^{64}Cu-PTSM uptake averaged over a 5 min interval from $t = 40$–45 min. Uptakes are divided by the total administered activity. Shown are data for the five unheated control tumours. In addition, Figure 7 displays the low activity ^{64}Cu-PTSM and early ^{64}Cu-ATSM data for a readily identifiable normal structure: the last 5 mm of the five animals' tails. The unheated control tumour and tail data are consistent with the early ^{64}Cu-ATSM uptake being approximately proportional to perfusion within a structure. A least squares linear fit is included in Figure 7.

The low activity ^{64}Cu-PTSM scan cannot be used to estimate perfusion in the heated tumours since an intervention that alters perfusion (hyperthermia) took place after the low activity scan. There is, however, another approximate measure of local perfusion after hyperthermia that can be compared with the early ^{64}CuATSM uptake. For the five tumours heated with ultrasound, the steady state applied ultrasound power needed to maintain target temperature is approximately proportional to the average perfusion per unit volume of tumour [45]. Figure 8 displays the early uptake (first 60 s) of ^{64}Cu-ATSM per cc of tumour vs. the steady state ultrasound power needed to maintain temperature at 41.5°C. As was the case for the unheated tumours and tails displayed in Figure 7, the early ^{64}Cu-ATSM uptake appears to be approximately proportional to a measure of local perfusion. It should be noted that the five animals heated with ultrasound in Figure 8 were the same five animals with low activity PTSM scans in Figure 7.

Self-normalized tumour uptake

With the above in mind, this study therefore normalizes for delivery of radiotracer to the tumour (i.e. local perfusion), by dividing the time-dependent radiotracer activity by the early activity averaged over the first minute after administration. This is referred to as 'self-normalized' time dependent activity. Figure 9 displays the average self-normalized activity for the 10 post-hyperthermia scans for the heated and control tumours for all 10 animals. The standard error is also displayed. The heated and control tumours separate by more than the sum of standard errors after 2 min ($p = 0.007$ at $t = 2$ min, $p < 0.001$ for $t > 5$ min; Gaussian distribution assumed for probabilities, two-tailed integration). If the variance for the 10 animals is representative, then a group of four would separate by more than the sum of standard errors ($SE_4 = SE_{10} \times (10/4)^{1/2}$) about 6 min after administration of radiotracer. This is consistent with what is seen in the sub-group analysis discussed below (see Figures 10 and 11).

Four of the animals had low activity ^{64}Cu-ATSM scans preceding hyperthermia. These four were heated with the conductive device. They provide an opportunity to directly compare ATSM scans before and after an intervention (hyperthermia) in the same tumour. Figure 10 demonstrates that, by 5 min after administration, the self-normalized activity is reduced significantly after hyperthermia ($p \leq 0.02$ for $t \geq 5$ min). As would be expected,

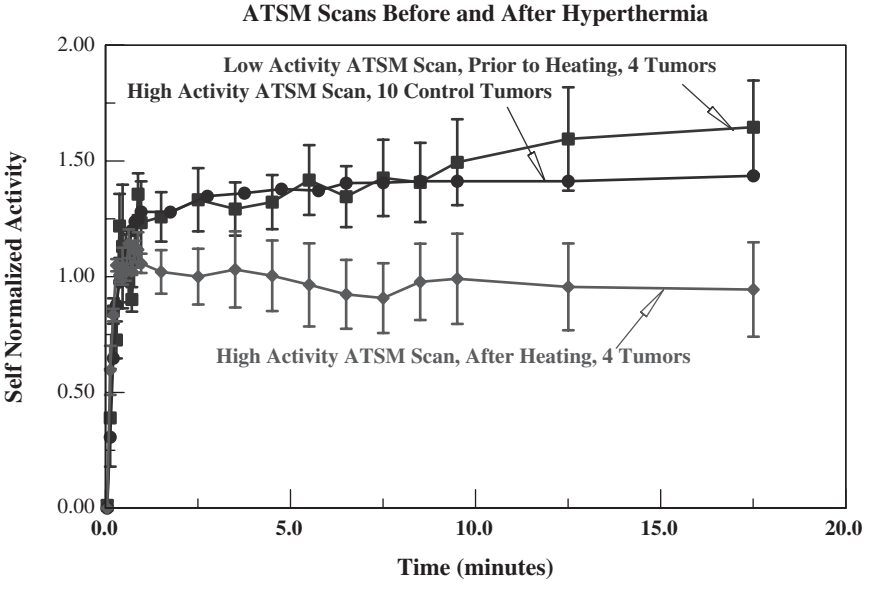

Figure 10. Data from the four animals who had low activity Cu-ATSM scans before heating. The self-normalized uptake (see Figure 9 and text) for the four heated tumours in the full activity Cu-ATSM scan is compared with the self-normalized uptake for the same tumours in the low activity scan, obtained immediately before hyperthermia. Because the number of tumours is smaller, standard errors are larger than in Figure 9. Also displayed is the self-normalized uptake from the full activity Cu-ATSM scans for all 10 control tumours (reproduced from Figure 9, standard error omitted for clarity), confirming that, before being heated, these four tumours were comparable to the unheated controls.

the pre-hyperthermia behaviour for these four tumours is indistinguishable from the 10 unheated control tumours, full activity scans. This confirms that, prior to hyperthermia, the heated tumours had oxygenation status that was similar to the control tumours. Following mild hyperthermia, there was significant reduction in the self-normalized ATSM activity in heated tumours, consistent with improved oxygenation.

Figure 11 displays the self-normalized ^{64}Cu-PTSM activity vs. time data averaged over 10 tumours for the last five mice. These were obtained from the low activity, pre-hyperthermia scans for these mice. Following the PTSM scan, hyperthermia was delivered with the ultrasound device. Comparison between the curves for heated tumours in Figures 10 and 11 confirms the equivalence between the ultrasound and conduction devices, since ultrasound heating was used for Figure 11 and conductive heating for Figure 10. The self-normalized ^{64}Cu-ATSM activity vs. time data in Figure 11 show that ATSM activity for the unheated control tumours lies mid-way between the PTSM activity and the ATSM activity for heated tumours. ^{64}Cu-PTSM would be expected to show the greatest retention of delivered radiotracer, because *in-vitro* studies show it is retained at the same level as Cu-ATSM in hypoxic cells but, unlike Cu-ATSM, that level does not drop in well oxygenated cells [25]. The heated tumours show the lowest self-normalized activity for Cu-ATSM, consistent with improved oxygenation. For the five mice in Figure 11, the self-normalized uptake for heated and control tumours separate by more than the sum of standard errors by 2 min ($p < 0.01$). The self-normalized uptake for PTSM and ATSM controls separate at ~10 min ($p = 0.03$).

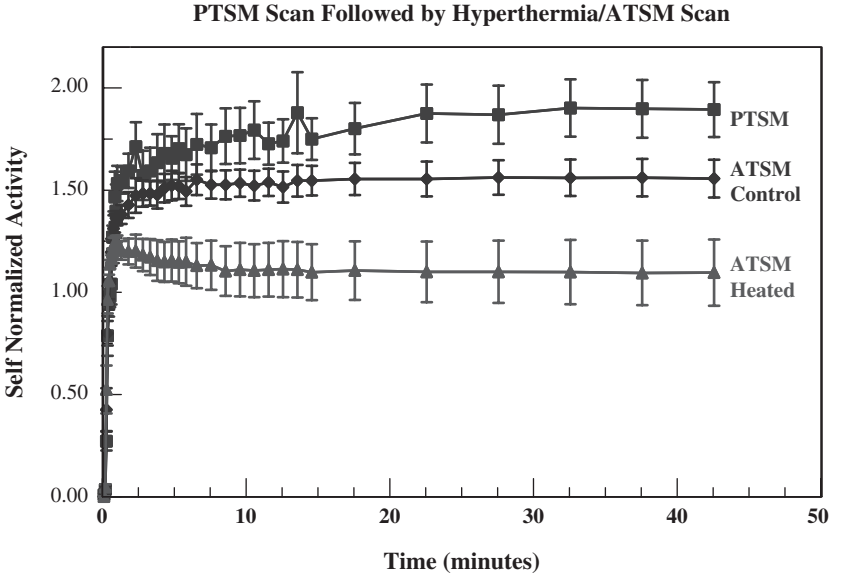

Figure 11. Data from the five mice who had low activity Cu-PTSM scans before heating and full activity Cu-ATSM scans. Self-normalized (see Figure 9, text) uptake for Cu-PTSM (averaged over 10 tumours, five mice) is compared with Cu-ATSM uptake in the five heated and control tumours. *In-vitro* studies show that radiotracer from Cu-PTSM is retained at the same level as Cu-ATSM in hypoxic cells but, unlike Cu-ATSM, that level does not drop in well oxygenated cells [25]. This is compatible with greater self-normalized uptake for Cu-PTSM. The heated tumours show the lowest self-normalized activity for Cu-ATSM, consistent with better oxygenation than the controls.

Duration of hyperthermia

As noted in the methods section, because two mice were heated at the same time, the time at or above 41°C varied. When one tumour reached 41°C ahead of the other, it was required that hyperthermia be continued until the second tumour was at or above 41°C for at least 30 min before initiating the full activity ^{64}Cu-ATSM scan. The total time at or above 41°C therefore ranged from 30–58 min, with a mean of 45 min. The Sapareto Dewey [46] equivalent time at 41.5°C (which is very strongly affected by relatively small temperature changes) ranged from 29–73 equivalent minutes with a mean of 44 equivalent minutes. Within this range, no association was found between duration of heating and ATSM scan findings. There were six tumours heated for less than 40 equivalent minutes at 41.5°C (sub-group mean 33 equivalent minutes). For these six, the self-normalized uptake from $t = 15$ to $t = 20$ min was 1.06 ± 0.13. For the four tumours heated more than 40 equivalent minutes (sub-group mean 60 equivalent minutes), the self-normalized ATSM uptake was 0.97 ± 0.19.

Post-hyperthermia pO_2 electrode readings and scan findings

Table I summarizes findings from the comparison of scans with pO_2 electrode readings. The profile tool was used to generate uptake as a function of time for 11–12 points along a narrow rectangle set to match, as closely as possible, the track to be surveyed with the needle probe. The self-normalized uptake for each point in the profile was the average uptake 10–15 min after radiotracer injection, divided by the uptake for the same point

Table I. Comparison of self-normalized uptake of ^{64}Cu-ATSM with pO_2 by needle electrode surveys, data from four mice with eight tumours (four heated, four controls), heating by ultrasound. The electrode data represent the average pO_2 obtained by successive 1 mm pullbacks over 11–12 points in a single needle track for each tumour, obtained after cessation of scanning and hyperthermia. Self-normalized uptake is averaged over the same number of spatial locations in a thin rectangle set as close as possible to match the needle track. Scan findings obtained during hyperthermia are from low administered activity injections, 30 min into the hyperthermia session. Scan findings after cessation of hyperthermia are from full administered activity injections performed immediately after (right mouse tumours) and 15 min after (left mouse) the end of hyperthermia. Fifteen minutes of image acquisition time was used for each scan and ~15 min was needed for each electrode survey. Time refers to the initiation of either scan or electrode survey. Standard errors represent scatter over the monitored spatial points.

	Time (min) after end of hyperthermia	Self-normalized uptake	pO_2 (mm Hg)	Number of spatial points	*p vs.* controls
Controls	X	1.20 ± 0.05	13.5 ± 2	45	X
R Heated	During hyperthermia	0.64 ± 0.06	X	24	<0.001
L Heated	During hyperthermia	0.75 ± 0.07	X	23	<0.001
R Heated	0	0.70 ± 0.05	X	24	<0.001
R Heated	~15	X	23 ± 2	24	<0.001
L Heated	15	1.06 ± 0.04	X	23	0.03
L Heated	~45	X	17.7 ± 3	23	NS

averaged over the first minute after injection. As with the data displayed in Figures 9–11, the self-normalized uptake in these experiments changed little after 5 min following administration of radiotracer.

The self-normalized uptake obtained beginning 15 min after the end of hyperthermia (heated tumours in the two left mice) was significantly higher than the self-normalized uptake for the same two tumours during hyperthermia (1.06 ± 0.04 vs. 0.75 ± 0.07, $p < 0.001$), although still significantly lower than the four control tumours (1.06 ± 0.04 vs. 1.20 ± 0.05, $p = 0.03$). The self-normalized uptake during hyperthermia was unchanged immediately after cessation of hyperthermia (heated tumours in the two right mice) and was significantly less than in unheated controls ($p < 0.001$).

The electrode surveys begun 15 min after end of hyperthermia (heated tumours in the two right mice) show significantly higher pO_2 than the control tumors (23 ± 2 vs. 13 ± 2 mm Hg). The electrode surveys ~45 min after the end of hyperthermia (heated tumours in the two left mice), show a pO_2 that is higher than controls, but not significantly so.

Direct comparison between pO_2 survey and self-normalized uptake for the same tumours shows that self-normalized uptake is anti-correlated with pO_2: increased oxygenation is associated with decreased self-normalized uptake. The two right tumours (scanned and surveyed as soon as possible after the end of hyperthermia) show decreased radiotracer retention (decreased self-normalized uptake) and increased pO_2 compared with controls. The effect in the two left tumours (scanned and surveyed after a longer interval) is not as great as the right tumours, but, again, pO_2 is greater and self-normalized uptake is less than controls.

Discussion

This study sought to identify a tool that could quickly (within a few minutes) discriminate the impact of mild hyperthermia on hypoxia imaging, without interrupting heating.

For Cu-ATSM PET scanning, the self-normalized uptake, defined above, appears to be one such tool. Being able to quickly discriminate the effects of hyperthermia on *in-vivo* tumour physiology may be helpful. It is known that other effects of hyperthermia can change rapidly with time; the short-term time dependence of effects on oxygenation is, however, presently unknown.

The cytotoxic effects of hyperthermia are strongly dependent on both time and temperature [46]. The fraction of cells surviving a cytotoxic thermal dose decreases exponentially with time and depends sharply on temperature. There is little direct cell kill from temperatures below 42°C maintained for times of ~1 h or less. Temperatures in the 41–42°C range will, however, produce significant heat induced radiosensitization if maintained for at least 1 h, if the heat and radiation are given simultaneously [31–38]. If heat and radiation are given sequentially, temperatures in the 41–42°C range must be maintained for substantially longer times (2–6 h, depending on the cell line) for the same level of heat induced radiosensitization [37]. As temperatures are increased above 42°C, the time needed for equivalent levels of either direct thermal cytotoxicity or heat induced radiosensitization drop sharply.

In addition to direct cellular effects from heat and heat plus radiation, hyperthermia can also affect the response of tumours by altering tumour physiology—particularly by impacting on tumour oxygenation. For temperatures below 42°C the physiologic effects may have a comparable or greater impact on tumour curability than direct cellular effects. For example, heat induced radiosensitization from 1 h at 41°C would be expected to reduce the surviving fraction from a 3 Gy radiation treatment by ~0.8 [38], which could also be achieved by converting ~20% of hypoxic cells into more sensitive normoxic cells. Since, in the clinic, minimum tumour temperatures are usually <42°C, optimizing the physiologic effects of mild hyperthermia may be of substantial import.

It is not well known to what extent the physiologic effects of hyperthermia vary with time: whether very short heating sessions are as effective as sessions lasting ~1 h and how rapidly these effects decay, once hyperthermia is discontinued. PET-based imaging is an approach that provides a non-invasive opportunity to obtain information from an entire tumour, without interrupting heating, if need be. Unlike some small animal imaging modalities, such as optical imaging or electron paramagnetic resonance, the photon energies with PET are sufficient to image deep-seated tumours in humans. This means findings in small animal models can be more directly applied to human subjects. However, PET scans in the clinic typically rely on images obtained ~1 h after administration. While this is generally sufficient for diagnostic or staging purposes, such a time window is too large to discriminate short-term or transitory effects of interventions.

The present study sought to obtain information from ^{64}Cu-ATSM PET scans that would discriminate between heated and control tumours in short periods of time (less than 10 min) with a moderate number of animals. The fact that radiotracer begins to be taken up and retained in hypoxic cells in a time scale of minutes (Figure 4) makes it a moiety that could, in principle, serve this purpose. This study initially considered kinetic modelling of uptake data. Typically this involves fitting tumour uptake to a multiple compartment model with four or more kinetic parameters. It was found, however, that over limited periods of time (<20 min) the information was too limited to avoid degeneracies (multiple solutions fitting the data equally well).

Because mild hyperthermia enhances tumour perfusion, relatively more radiotracer is delivered after mild hyperthermia than without heating. For this reason, the self-normalized uptake was evaluated (absolute uptake divided by average uptake over the first minute following radiotracer administration). Figures 7 and 8 are consistent

with the uptake over the first minute being approximately proportional to perfusion in the tumour. As seen in Figure 9, the self-normalized uptake averaged over 10 animals becomes significantly less in heated tumours by 2 min ($p = 0.007$). If the scatter for 10 animals is representative, then the standard error for a sample of four animals would separate by the sum of standard errors by ~6 min. This is consistent with what, in fact, is seen when sub-sets of the overall cohort are looked at (Figures 10 and 11). Because the self-normalized uptake of Cu-ATSM discriminates between modest numbers of heated and control tumours within a time scale of minutes, it is felt that it provides a tool that can be used to evaluate the effects of short hyperthermia sessions and how they evolve after hyperthermia is stopped.

The comparison between self-normalized ^{64}Cu-PTSM and ^{64}Cu-ATSM uptakes, such as shown in Figure 11 suggests that information from these two scans might be used to determine the fraction of hypoxic but viable cells within a tumour. This is because Cu-PTSM uptake is independent of oxygenation status, while Cu-ATSM uptake is equal to that of Cu-PTSM for hypoxic cells but drops sharply above ~5 mm Hg—hence the difference between the two reflects the portion of viable cells that are not hypoxic. The authors also plan to explore this in future investigations.

The comparison between post-hyperthermia scans and needle electrode pO_2 surveys shows a good association between increasing pO_2 and decreasing self-normalized uptake (Table I). These studies also suggest that (for this thermal dose in this tumour model) the improvement in tumour oxygenation degrades substantially between ~15–45 min after hyperthermia is stopped. Although others have found that the effect of hyperthermia on tumour oxygenation persists for a long time [2, 7], these studies have heated portions of the tumour to substantially higher temperatures than 41.5°C, which could lead to more thermal injury and therefore longer lasting effects on the tumour. Note that it may be of clinical benefit to have a thermal effect on tumour oxygenation that reverses shortly after the hyperthermia session. There would be less inter-fraction repopulation, if hypoxic regions revert back to being hypoxic between treatments. The authors will be evaluating the impact of thermal dose on the time dependence of tumour physiology in future studies.

Recently, Matsumoto et al. [47] reported results of experiments in which mice with implanted squamous cell carcinomas underwent two scans, with a hypoxia directed intervention (Carbogen breathing) between scans. They could not detect a difference between the pre- and post-intervention Cu-ATSM scans. This is in contrast to the data presented in Figure 10 of this paper. Figure 10 accounted for the effects of an intervention (hyperthermia) on tumour perfusion by using the self-normalized uptake. Correcting for the effects on perfusion is particularly important for a scan moiety like Cu-ATSM that begins to equilibrate with hypoxic tissue in a time scale of minutes. A scanning moiety, like F-Misonidazole, that takes longer to bind, may ultimately achieve greater differences between hypoxic and non-hypoxic zones—and, therefore, the ultimate difference between pre- and post-intervention scans may be easier to discriminate. However, the long time to equilibrium makes it unsuitable for discriminating short time effects.

It is also important that the pre-hyperthermia (or other intervention) scan be conducted with a lower administered activity than the post-intervention scan. In the Matsumoto et al. study, the two scans were of equal activity. Therefore, continued evolution of the residual uptake from the first scan could potentially introduce ~10–20% effects in the second scan. This, in turn, could obscure effects like those seen in Figure 10.

Acknowledgement

It is a pleasure to acknowledge useful discussions with Jason Lewis, Deborah McCarthy and Richard Laforest. Research supported in part by NIH grants 1R24 CA86307, 1R24 CA83060, R01 CA63121, R01 CA71638-08.

References

1. Feldmann HJ, Molls M, Fuller J, Stuben G, Sack H. Changes in oxygenation patterns of locally advanced recurrent tumors under thermoradiotherapy. Adv Exp Med Biol 1994;345:479–483.
2. Brizel DM, Scully SP, Harrelson JM, Layfield LJ, Dodge RK, Charles HC, Samulski TV, Prosnitz LR, Dewhirst MW. Radiation therapy and hyperthermia improve the oxygenation of human soft tissue sarcomas. Cancer Res 1996;56:5347–5350.
3. Iwata K, Shakil A, Hur WJ, Makepeace CM, Griffin RJ, Song CW. Tumour pO_2 can be increased markedly by mild hyperthermia. Br J Cancer Suppl 1996;27:S217–S221.
4. Horsman MR, Overgaard J. Can mild hyperthermia improve tumour oxygenation? Int J Hyperthermia 1997;13:141–147.
5. Song CW, Shakil A, Griffin RJ, Okajima K. Improvement of tumor oxygenation status by mild temperature hyperthermia alone or in combination with carbogen. Semin Oncol 1997;24:626–632.
6. Shakil A, Osborn JL, Song CW. Changes in oxygenation status and blood flow in a rat tumor model by mild temperature hyperthermia. Int J Radiat Oncol Biol Phys 1999;43:859–865.
7. Vujaskovic Z, Poulson JM, Gaskin AA, Thrall DE, Page RL, Charles HC, MacFall JR, Brizel DM, Meyer RE, Prescott DM, Samulski TV, Dewhirst MW. Temperature-dependent changes in physiologic parameters of spontaneous canine soft tissue sarcomas after combined radiotherapy and hyperthermia treatment. Int J Radiat Oncol Biol Phys 2000;46:179–185.
8. Song CW, Shakil A, Osborn JL, Iwata K. Tumour oxygenation is increased by hyperthermia at mild temperatures. Int J Hyperthermia 1996;12:367–373.
9. Griffin RJ, Okajima K, Song CW. The optimal combination of hyperthermia and carbogen breathing to increase tumor oxygenation and radiation response. Int J Radiat Oncol Biol Phys 1998;42:865–869.
10. Zwart A, Kwant G, Oeseburg B, Zijlstra WG. Human whole-blood oxygen affinity: Effect of temperature. J Appl Physiol 1984;57:429–434.
11. Roszinski S, Wiedemann G, Jiang SZ, Baretton G, Wagner T, Weiss C. Effects of hyperthermia and/or hyperglycemia on pH and pO_2 in well oxygenated xenotransplanted human sarcoma. Int J Radiat Oncol Biol Phys 1991;20:1273–1280.
12. Kallinowski F, Zander R, Hoeckel M, Vaupel P. Tumor tissue oxygenation as evaluated by computerized-pO_2-histography. Int J Radiat Oncol Biol Phys 1990;19:953–961.
13. Vaupel P, Schlenger K, Knoop C, Hockel M. Oxygenation of human tumors: Evaluation of tissue oxygen distribution in breast cancers by computerized O_2 tension measurements. Cancer Res 1991;51:3316–3322.
14. Rasey JS, Koh WJ, Evans ML, Peterson LM, Lewellen TK, Graham MM, Krohn KA. Quantifying regional hypoxia in human tumors with positron emission tomography of [18F]fluoromisonidazole: A pretherapy study of 37 patients. Int J Radiat Oncol Biol Phys 1996;36:417–428.
15. Chapman JD, Engelhardt EL, Stobbe CC, Schneider RF, Hanks GE. Measuring hypoxia and predicting tumor radioresistance with nuclear medicine assays. Radiother Oncol 1998;46:229–237.
16. Al-Hallaq HA, Zamora M, Fish BL, Farrell A, Moulder JE, Karczmar GS. MRI measurements correctly predict the relative effects of tumor oxygenating agents on hypoxic fraction in rodent BA1112 tumors. Int J Radiat Oncol Biol Phys 2000;47:481–488.
17. Cooper RA, Carrington BM, Loncaster JA, Todd SM, Davidson SE, Logue JP, Luthra AD, Jones AP, Stratford I, Hunter RD, West CM. Tumour oxygenation levels correlate with dynamic contrast-enhanced magnetic resonance imaging parameters in carcinoma of the cervix. Radiother Oncol 2000;57:53–59.
18. Evans SM, Kachur AV, Shiue CY, Hustinx R, Jenkins WT, Shive GG, Karp JS, Alavi A, Lord EM, Dolbier Jr WR, Koch CJ. Noninvasive detection of tumor hypoxia using the 2-nitroimidazole [18F]EF1. J Nucl Med 2000;41:327–336.
19. Chapman JD, Schneider RF, Urbain JL, Hanks GE. Single-photon emission computed tomography and positron-emission tomography assays for tissue oxygenation. Semin Radiat Oncol 2001;11:47–57.

20. Krishna MC, Subramanian S, Kuppusamy P, Mitchell JB. Magnetic resonance imaging for *in vivo* assessment of tissue oxygen concentration. Semin Radiat Oncol 2001;11:58–69.
21. Lewis JS, Sharp TL, Laforest R, Fujibayashi Y, Welch MJ. Tumor uptake of copper-diacetyl-Bis(N^4-methylthiosemicarbazone): Effect of changes in tissue oxygenation. J Nucl Med 2001;42:655–661.
22. Yamada KI, Kuppusamy P, English S, Yoo J, Irie A, Subramanian S, Mitchell JB, Krishna MC. Feasibility and assessment of non-invasive *in vivo* redox status using electron paramagnetic resonance imaging. Acta Radiol 2002;43:433–440.
23. Elas M, Williams BB, Parasca A, Mailer C, Pelizzari CA, Lewis MA, River JN, Karczmar GS, Barth ED, Halpern HJ. Quantitative tumor oxymetric images from 4D electron paramagnetic resonance imaging (EPRI): Methodology and comparison with blood oxygen level-dependent (BOLD) MRI. Magn Reson Med 2003;49:682–691.
24. Fujibayashi Y, Taniuch H, Yonekura Y, Ohtani H, Konishi J, Yokoyama A. Copper-62-ATSM: A new hypoxia imaging agent with high membrane permeability and low redox potential. J Nucl Med 1997;38:1155–1160.
25. Lewis JS, McCarthy DW, McCarthy TJ, Fujibayashi Y, Welch MJ. Evaluation of 64Cu-ATSM *in vitro* and *in vivo* in a hypoxic tumor model. J Nucl Med 1999;40:177–183.
26. McCarthy DW, Bass LA, Cutler PD, Shefer RE, Klinkowstein RE, Herrero P, Lewis JS, Cutler CS, Anderson CJ, Welch MJ. High purity production and potential applications of copper-60 and copper-61. Nucl Med Biol 1999;26:351–358.
27. Chao KS, Bosch WR, Mutic S, Lewis JS, Dehdashti F, Mintun MA, Dempsey JF, Perez CA, Purdy JA, Welch MJ. A novel approach to overcome hypoxic tumor resistance: Cu-ATSM-guided intensity-modulated radiation therapy. Int J Radiat Oncol Biol Phys 2001;49:1171–1182.
28. Dehdashti F, Grigsby PW, Mintun MA, Lewis JS, Siegel BA, Welch MJ. Assessing tumor hypoxia in cervical cancer by positron emission tomography with 60Cu-ATSM: Relationship to therapeutic response – a preliminary report. Int J Radiat Oncol Biol Phys 2003;55:1233–1238.
29. Dehdashti F, Mintun MA, Lewis JS, Bradley J, Govindan R, Laforest R, Welch MJ, Siegel BA. *In vivo* assessment of tumor hypoxia in lung cancer with 60Cu-ATSM. Eur J Nucl Med Mol Imaging 2003;30:844–850. Epub 2003 Apr 2012.
30. McCarthy DW, Shefer RE, Klinkowstein RE, Bass LA, Margeneau WH, Cutler CS, Anderson CJ, Welch MJ. Efficient production of high specific activity 64Cu using a biomedical cyclotron. Nucl Med Biol 1997;24:35–43.
31. Overgaard J. Simultaneous and sequential hyperthermia and radiation treatment of an experimental tumor and its surrounding normal tissue *in vivo*. Int J Radiat Oncol Biol Phys 1980;6:1507–1517.
32. Overgaard J. The current and potential role of hyperthermia in radiotherapy. Int J Radiat Oncol Biol Phys 1989;16:535–549.
33. Steeves RA, Murray TG, Moros EG, Boldt HC, Mieler WF, Paliwal BR. Concurrent ferromagnetic hyperthermia and 125I brachytherapy in a rabbit choroidal melanoma model. Int J Hyperthermia 1992;8:443–449.
34. Dewey WC. Arrhenius relationships from the molecule and cell to the clinic. Int J Hyperthermia 1994;10:457–483.
35. Steeves RA, Tompkins DT, Nash RN, Blair JR, Gentry LL, Paliwal BR, Murray TG, Mieler WF. Thermoradiotherapy of intraocular tumors in an animal model: Concurrent vs. sequential brachytherapy and ferromagnetic hyperthermia. Int J Radiat Oncol Biol Phys 1995;33:659–662.
36. Myerson RJ, Straube WL, Moros EG, Emami BN, Lee HK, Perez CA, Taylor ME. Simultaneous superficial hyperthermia and external radiotherapy: Report of thermal dosimetry and tolerance to treatment. Int J Hyperthermia 1999;15:251–266.
37. Xu M, Myerson RJ, Straube WL, Moros EG, Lagroye I, Wang LL, Lee JT, Roti Roti JL. Radiosensitization of heat resistant human tumour cells by 1 hour at 41.1°C and its effect on DNA repair. Int J Hyperthermia 2002;18:385–403.
38. Myerson RJ, Roti Roti JL, Moros EG, Straube WL, Xu M. Modelling heat-induced radiosensitization: Clinical implications. Int J Hyperthermia 2004;20:201–212.
39. Moros EG, Straube WL, Klein EE, Maurath J, Myerson RJ. Clinical system for simultaneous external superficial microwave hyperthermia and cobalt-60 radiation. Int J Hyperthermia 1995;11:11–26.
40. Straube WL, Moros EG, Low DA, Klein EE, Willcut VM, Myerson RJ. An ultrasound system for simultaneous ultrasound hyperthermia and photon beam irradiation. Int J Radiat Oncol Biol Phys 1996;36:1189–1200.

41. Singh AK, Moros EG, Novak P, Straube W, Zeug A, Locke JE, Myerson RJ. MicroPET-compatible, small animal hyperthermia ultrasound system (SAHUS) for sustainable, collimated and controlled hyperthermia of subcutaneously implanted tumours. Int J Hyperthermia 2004;20:32–44.
42. Rockwell S. *In vivo–in vitro* tumour cell lines: Characteristics and limitations as models for human cancer. Br J Cancer Suppl 1980;41:118–122.
43. Moulder JE, Rockwell S. Hypoxic fractions of solid tumors: Experimental techniques, methods of analysis, and a survey of existing data. Int J Radiat Oncol Biol Phys 1984;10:695–712.
44. Shibamoto Y, Nishimoto S, Mi F, Sasai K, Kagiya T, Abe M. Evaluation of various types of new hypoxic cell sensitizers using the EMT6 single cell-spheroid-solid tumour system. Int J Radiat Biol Relat Stud Phys Chem Med 1987;52:347–357.
45. Myerson RJ, Emami BN, Perez CA, Straube W, Leybovich L, Von D. Equilibrium temperature distributions in uniform phantoms for superficial microwave applicators: Implications for temperature-based standards of applicator adequacy. Int J Hyperthermia 1992;8:11–21.
46. Sapareto SA, Dewey WC. Thermal dose determination in cancer therapy. Int J Radiat Oncol Biol Phys 1984;10:787–800.
47. Matsumoto K, Seidel J, Szajek L, Krishna M, Green M, Eckelman W, Bacharach S, Mitchell J. Imaging hypoxia in murine squamous cell carcinoma using Cu 64-ATSM (Abstract #MIT-1074-282034). Radiation Research Society Annual Meeting. St. Louis, MO; 24–27 April 2004.